RSC Advances

PAPER

View Article Online
View Journal | View Issue

Cite this: *RSC Adv.*, 2026, **16**, 657

Multifunctional Cu-DEOD porous polymeric nanocomposite for broad-spectrum biomedical applications

Hadil Faris Alotaibi,[a] Fadhil Faez Sead,[b] Farag M. A. Altalbawy,[c] Nawfal Yousif,[d] Ahmed Salih Sahib,[ef] Zahraa Saad Abdulali,[g] Mariem Alwan,[h] Mahmood Jasem,[i] Hiba Mushtaq,[j] Adama Faye *[k] and Aseel Smerat[l]

A novel porous polymeric (PPN) was engineered by integrating Dabrafenib, Enrofloxacin, Dipicolinic acid, Oxidized Pectin, and copper (Cu-DEOD PPN), resulting in a porous polymeric architecture with enhanced bioactivity. The synergistic combination of therapeutic and antimicrobial agents within a stable, biocompatible matrix endowed the nanocomposite with multifunctional properties, including anticancer, antibacterial, antioxidant, and analgesic effects. Structural characterization confirmed uniform dispersion of active constituents and a well-defined porous network. Key findings demonstrated an average particle size of 90 nm, and biological evaluation demonstrated significant efficacy: minimum inhibitory concentration (MIC) 2–8 μg mL^{-1}, minimum bactericidal concentration (MBC) 4–16 μg mL^{-1}, and half-maximal inhibitory concentration (IC_{50}) 165 μg mL^{-1} against NCI-H1299, and and up to 86% DPPH radical inhibition. The multifunctional performance of Cu-DEOD PPN highlights its potential as a versatile therapeutic platform for oncology, infection management, oxidative stress mitigation, and pain relief, providing a framework for the design of next-generation bioactive nanomaterials. This study emphasizes a strategic approach to developing multifunctional nanocomposites that simultaneously combine therapeutic potency, biocompatibility, and structural integrity, offering promising applications in pharmaceutical and biomedical research.

Received 31st October 2025
Accepted 8th December 2025

DOI: 10.1039/d5ra08371k

rsc.li/rsc-advances

Introduction

Cancer remains one of the most challenging diseases worldwide due to its multifactorial pathogenesis, heterogeneity, and the complex interplay between tumor cells and their surrounding microenvironment.[1] Conventional chemotherapeutic strategies, although effective in some cases, are often limited by systemic toxicity, multidrug resistance, poor selectivity, and severe adverse effects that compromise patient quality of life.[2] Moreover, patients undergoing cancer therapy are particularly vulnerable to secondary bacterial infections, oxidative stress, and inflammation, which further complicate treatment outcomes.[3] In this context, the development of multifunctional therapeutic systems that integrate anticancer, antimicrobial, antioxidant, and analgesic activities within a single platform represents a highly desirable and forward-looking approach in precision medicine.

Nanotechnology has emerged as a powerful strategy to overcome these challenges by enabling site-specific drug delivery, controlled release, improved bioavailability, and the co-delivery of multiple therapeutic agents with synergistic activity.[4,5] The rational design of nanocomposites allows for the simultaneous targeting of cancer cells while addressing associated complications such as infections, oxidative damage, and treatment-induced pain.[6] Biopolymer-based nanostructures, in particular, offer excellent biocompatibility, biodegradability, and modifiability, making them ideal candidates for drug delivery systems.[7] By combining bioactive molecules with structurally supportive and functional components, it becomes

[a]*Department of Pharmaceutical Sciences, College of Pharmacy, Princess Nourah Bint AbdulRahman University, Riyadh 11671, Saudi Arabia*
[b]*Department of Dentistry, College of Dentistry, The Islamic University, Najaf, Iraq*
[c]*Department of Chemistry, University College of Duba, University of Tabuk, Tabuk, Saudi Arabia*
[d]*Department of Radiology Techniques, Health and Medical Techniques College, Alnoor University, Nineveh, Iraq*
[e]*College of Pharmacy, Ahl Al Bayt University, Iraq*
[f]*Department of Pharmacology and Toxicology, College of Pharmacy, University of Kerbala, Iraq*
[g]*College of Health and Medical Technology, National University of Science and Technology, Dhi Qar, 64001, Iraq*
[h]*Pharmacy College, Al-Farahidi University, Iraq*
[i]*Department of Pharmacy, Al-Zahrawi University College, Karbala, Iraq*
[j]*Gilgamesh Ahliya University, Baghdad, Iraq*
[k]*Department of Pharmacy, Faculty of Medicine, Pharmacy and Odonto-Stomatology, University of Ziguinchor, Ziguinchor, Senegal. E-mail: khrshdmuzammil@gmail.com*
[l]*Hourani Center for Applied Scientific Research, Al-Ahliyya Amman University, Amman 19328, Jordan*

possible to engineer multifunctional nanoplatforms with unique therapeutic advantages.[8]

In the present work, we report the design and synthesis of a novel nanocomposite system composed of four complementary components: Dabrafenib, Enrofloxacin, Dipicolinic acid, and oxidized pectin. Each constituent contributes distinct therapeutic or structural functionalities, thereby enhancing the overall performance of the system.

Unlike earlier nanocomposites that typically focus on one or two therapeutic functions, in this design each constituent was selected based on a defined functional purpose, Dabrafenib for selective kinase inhibition, Enrofloxacin for broad-spectrum antimicrobial protection during immunocompromised states, dipicolinic acid as a chelating/stabilizing ligand for coordination around Cu^{2+} centers, and oxidized pectin as a reactive and biocompatible matrix providing aldehyde groups for covalent linking. Their combination enables a unified platform capable of simultaneously addressing tumor progression, infection risk, and oxidative imbalance. This integrated multifunctionality distinguishes the present system from previously published approaches and broadens the potential therapeutic relevance of polymer–metal hybrid platforms.

The integration of these four components into a unified nanocomposite is designed to provide several therapeutic advantages. First, the system delivers targeted anticancer effects by Dabrafenib directly within tumor sites, thereby reducing systemic toxicity and improving efficacy.[9] Second, the incorporation of Enrofloxacin ensures antimicrobial protection, particularly against opportunistic infections that frequently accompany cancer treatment.[10] Third, Dipicolinic acid contributes not only to structural stabilization but also to the modulation of oxidative stress, potentially enhancing the antioxidant capacity of the formulation.[11] Finally, the oxidized pectin matrix provides a biocompatible, biodegradable scaffold that facilitates sustained release, enhances cellular uptake, and may contribute to analgesic effects through modulation of inflammatory pathways.[12] Collectively, this design enables a multifunctional approach to cancer therapy that addresses tumor progression while simultaneously managing infection, oxidative stress, and treatment-associated pain.

From a formulation perspective, oxidized pectin and dipicolinic acid provide unique advantages in the assembly of nanocomposites. The reactive aldehyde and carboxyl groups introduced during pectin oxidation allow efficient conjugation with small-molecule drugs and stabilizing ligands.[13]

Although various nanocomposites systems have been proposed for biomedical applications[14] such for cancer therapy,[15] antimicrobial,[16,17] and antioxidant,[18] few have explored the combined use of a molecularly targeted anticancer drug (Dabrafenib), a fluoroquinolone antibiotic (Enrofloxacin), a chelating and stabilizing agent (Dipicolinic acid), and a biopolymeric matrix (oxidized pectin) within a single nanoplatform. The integration of these agents not only allows for synergistic therapeutic effects but also addresses several clinical challenges in cancer management, including infection control, oxidative stress reduction, and pain mitigation. To the best of our knowledge, this is the first study to develop such a multifunctional nanocomposite with simultaneous anticancer, antimicrobial, antioxidant, and analgesic properties.

In contrast to previously reported copper-polymer systems or multi-agent nanocomposites, no prior study has integrated a targeted anticancer drug, a broad-spectrum antibiotic, a metal-chelating stabilizer, and a reactive biopolymeric matrix into a single coordinated framework. This work therefore introduces a unified multifunctional platform that simultaneously addresses tumor inhibition, infection control, oxidative imbalance, and controlled drug release, representing a level of integration not achieved in earlier studies.

Results and discussion

Synthesis of the Cu-DEOD PPN

The Cu-DEOD PPN was obtained through a sonochemical route that integrated copper(II) nitrate, dipicolinic acid, enrofloxacin, oxidized pectin, and dabrafenib. First, oxidation of pectin introduced aldehyde functionalities, according to previous studies (Scheme 1).[19]

The Cu^{2+} ions coordinated with dipicolinic acid, enrofloxacin, and oxidized pectin to (Scheme 2) generate a MOF-like architecture (Cu-DEO PPN).

The aldehyde groups of oxidized pectin provided anchoring sites for dabrafenib conjugation, and according to Scheme 3, the Cu-DEOD PPN (dipicolinic acid/enrofloxacin/oxidized pectin/dabrafenib) was synthesized.

The Cu-DEOD PPN was characterized by Fourier Transform Infrared Spectroscopy (FT-IR), X-ray diffraction (XRD) pattern, X-ray photoelectron (XPS) spectroscopy, scanning electron microscope (SEM)/transmission electron microscopy (TEM) images, dynamic light scattering (DLS) diagram, Thermogravimetric (TGA) analysis, and Brunauer–Emmett–Teller (BET) theory.

FT-IR analysis was conducted to confirm the incorporation of all components into the hybrid framework and to identify the key coordination and functional–group interactions. The FTIR spectrum of the Cu-DEOD PPN in Fig. 1, exhibits several characteristic absorption bands that confirm the successful integration of all components into a single hybrid framework. An absorption around 3300 cm^{-1} corresponds to N–H stretching from amide and sulfonamide groups. The broadening and partial red-shift of this signal compared with the free precursors indicate the establishment of strong hydrogen bonding and possible coordination with Cu(II) centers. Weak to medium absorptions at 2950–2850 cm^{-1} are assigned to aliphatic C–H

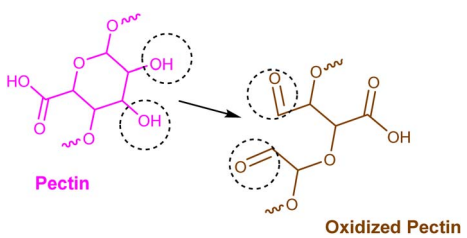

Scheme 1 Synthesis of oxidized pectin using pectin.

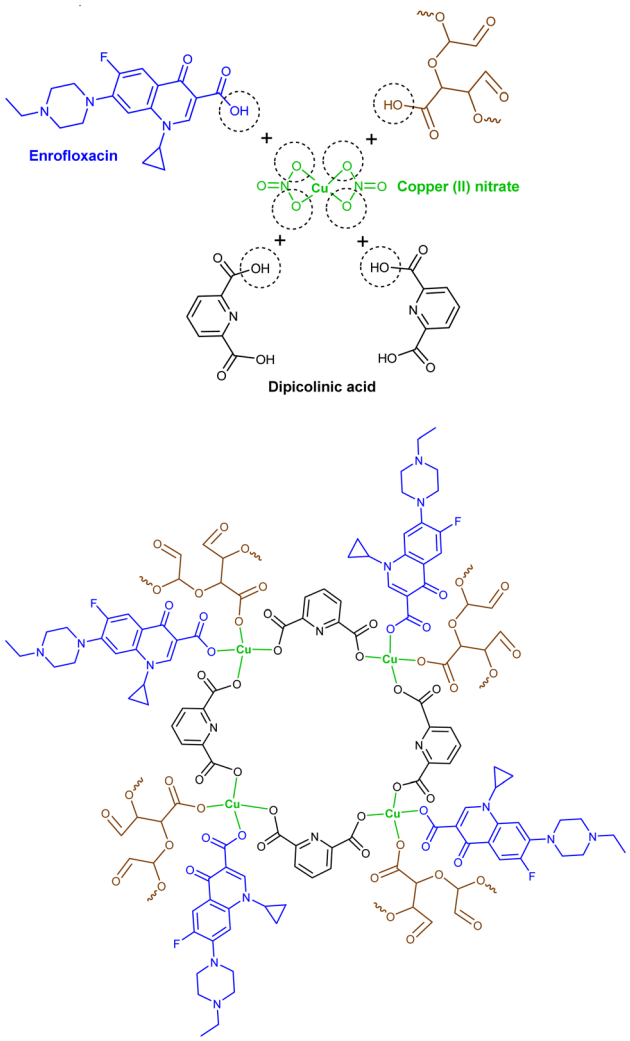

Scheme 2 Synthesis of Cu-DEO PPN using dipicolinic acid, enrofloxacin, and oxidized pectin.

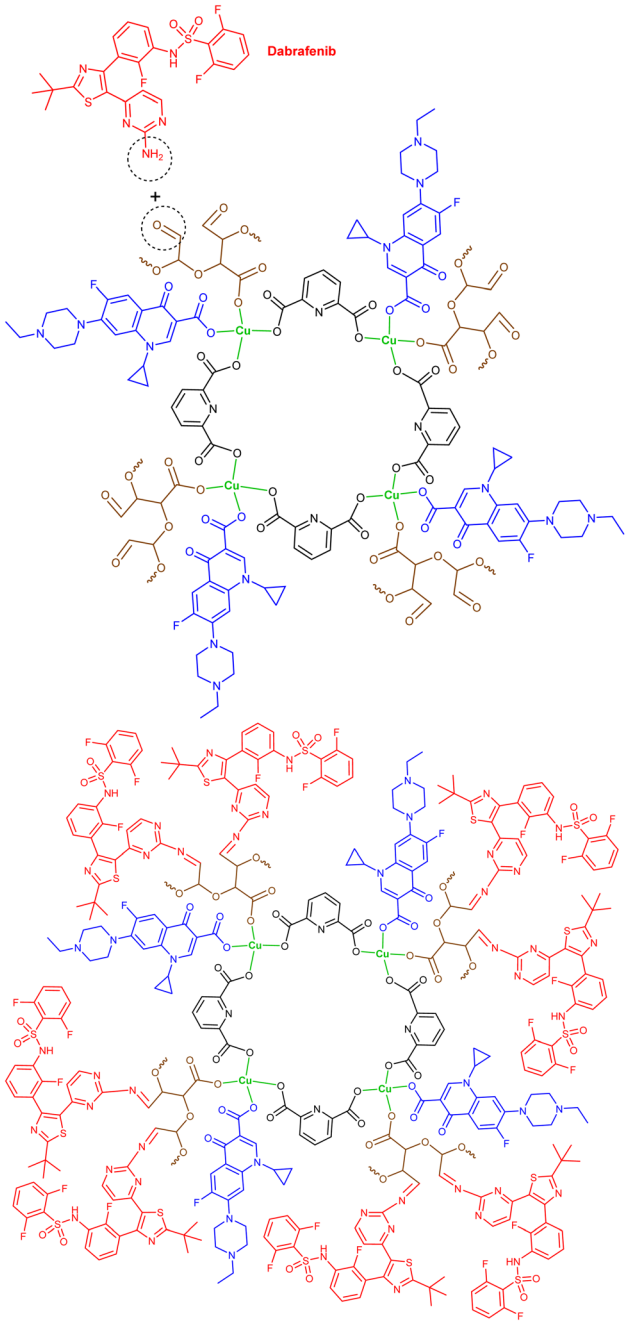

Scheme 3 Synthesis of Cu-DEOD PPN using Cu-DEO PPN and dabrafenib.

stretching vibrations originating from the alkyl moieties of the drug molecules and the polysaccharide scaffold.[20]

A sharp and intense band at 1720 cm^{-1} is attributed to C=O stretching of carboxylic acid and ester groups. The displacement of this band toward lower wavenumbers compared to the pure components suggests partial coordination of carboxyl groups to copper ions.[21] An additional band at 1650 cm^{-1} corresponds to the amide vibration and conjugated C=C stretching, while the absorption near 1590 cm^{-1} can be associated with aromatic C=C vibrations and asymmetric stretching of coordinated carboxylates.[22] Symmetric carboxylate stretching modes appear at 1380–1450 cm^{-1}, and the observed $\Delta\nu$ between asymmetric and symmetric bands supports a predominantly bidentate coordination pattern of dipicolinic acid.[23]

Strong absorptions around 1250 cm^{-1} are assigned to S=O stretching of sulfonyl groups[24] and C–O stretching of esters and ethers.[25] Additional strong features between 1150 and 1020 cm^{-1} are linked to C–F stretching vibrations of fluorinated aromatic groups and C–O–C vibrations of the oxidized pectin backbone.[26] The out-of-plane aromatic C–H bending observed around 840 cm^{-1} further confirms the presence of substituted aromatic rings from Dabrafenib and Enrofloxacin.[27]

In the low-frequency region, distinct new absorption appear at 650 cm^{-1}. The band near 650 cm^{-1} is characteristic of Cu–O stretching vibrations, indicating coordination of copper ions with carboxylate oxygen atoms of enrofloxacin, oxidized pectin and dipicolinic acid.[28]

XRD measurements were performed to evaluate the crystalline–amorphous characteristics of the composite and to identify

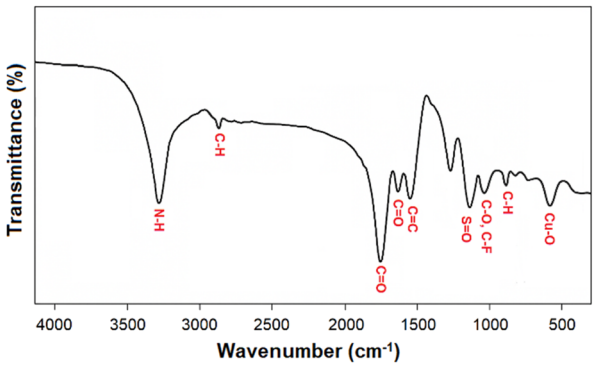

Fig. 1 Fourier Transform Infrared Spectroscopy (FTIR) of Cu-DEOD PPN.

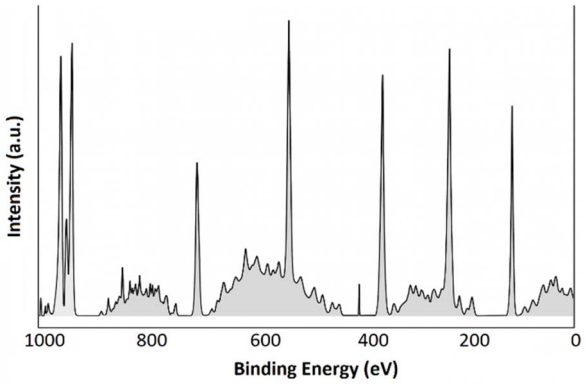

Fig. 3 X-ray photoelectron spectroscopy (XPS) of Cu-DEOD PPN.

the copper-based domains formed within the polymeric network. The XRD pattern for the Cu-DEOD PPN to (Fig. 2) indicates a predominantly amorphous biopolymeric matrix with embedded nanocrystalline copper oxide domains. A broad, low-intensity halo centered at approximately 20–24° 2θ is characteristic of the oxidized pectin scaffold and reflects the disordered polysaccharide network and reduced long-range order after oxidation and crosslinking. Superimposed on this amorphous background are sharper diffraction peaks that correspond to crystalline copper oxide (CuO, tenorite) and minor ordered domains attributable to molecular stacking in the drug components.[29,30]

The most prominent crystalline reflections are at $2\theta \approx 32.4°$, 35.5°, 38.8°, 48.7°, 61.4° and 66.4°. These peaks can be indexed to the monoclinic CuO phase (tenorite) and are commonly assigned to the (110), (11-1), (111), (20-2), (020), and (11-3) crystallographic planes. The presence of these specific reflections provides direct evidence for Cu–O bond formation in a crystalline oxide environment and supports the hypothesis that copper centers in the composite aggregate into nanoscale oxide domains during synthesis or post-synthesis drying/thermal treatments. This pattern is consistent with previously reported CuO nanocrystalline domains.[31,32]

XPS analysis was used to determine the surface elemental composition and the oxidation state of copper within the nanocomposite. The XPS spectroscopy (Fig. 3) was used to predict the surface chemical composition of the Cu-DEOD PPN containing copper. The survey spectrum exhibits distinct signals for S 2p signal at ~168.5 eV, C 1s (285.0 eV), N 1s (400.0 eV), O 1s (533.0 eV), F 1s (687 eV), and Cu 2p, confirming the presence of all expected elements.

High-resolution Cu 2p spectra display the characteristic Cu $2p_{3/2}$ peak at 932.6 eV and Cu $2p_{1/2}$ at 952.4 eV, together with shake-up satellites around 940.8 eV and 962.0 eV. These features are diagnostic of Cu(II) species (*e.g.*, CuO-like environments) and indicate that copper exists predominantly in the oxidized state within the composite.[33]

The O 1s region can be deconvoluted into three main contributions: lattice oxygen of Cu–O bonds at 530.1 eV, coordinated carboxylate/carbonyl oxygen at 531.5 eV, and higher-energy hydroxyl/C–O groups near 533.0 eV from the

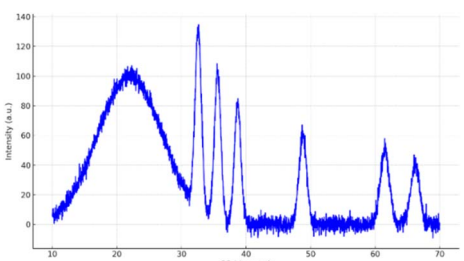

Fig. 2 X-ray diffraction (XRD) pattern of Cu-DEOD PPN.

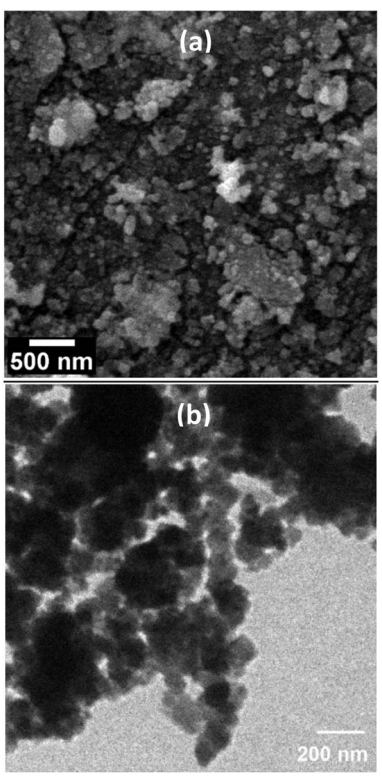

Fig. 4 SEM (a) and TEM (b) of Cu-DEOD PPN.

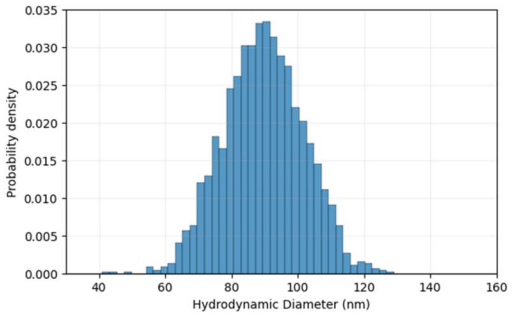

Fig. 5 Dynamic light scattering (DLS) of Cu-DEOD PPN.

polysaccharide framework. These components confirm that copper interacts primarily with oxygen donors.[34]

SEM and TEM imaging were employed to examine particle morphology, size distribution, and the structural uniformity of the synthesized nanocomposite. The SEM (Fig. 4a) images revealed nearly spherical to polyhedral nanoparticles with smooth surfaces, while TEM (Fig. 4b) demonstrated uniform particle distribution with average diameters below 100 nm. TEM highlighted lattice fringes corresponding to crystalline domains, and selected area electron diffraction (SAED) patterns supported the XRD observations.

DLS measurements were carried out to determine the hydrodynamic particle size, colloidal stability, and dispersion quality of the nanocomposite. The DLS (Fig. 5) measurements reported a mean hydrodynamic size of 90 nm with a low polydispersity index (0.2), confirming excellent dispersion. Zeta potential analysis yielded a negative surface charge (−25 mV), indicative of good colloidal stability. Size monitoring over seven days in phosphate buffered saline and serum-containing medium showed minimal aggregation, suggesting strong stability under physiological conditions.

TGA analysis was conducted to assess the thermal stability of the composite and to identify the sequential degradation behavior of its organic and inorganic components. The TGA analysis (Fig. 6) of the Cu-DEOD PPN displayed a multi-step weight loss profile, which reflects the sequential decomposition of its organic and inorganic components. An initial minor weight loss (3–5%) occurred below 120 °C, attributed to the evaporation of adsorbed moisture and loosely bound solvents. A more pronounced weight loss (15%) was observed between 280–360 °C, corresponding to the degradation of oxidized pectin chains and partial decomposition of dipicolinic acid. The major decomposition stage occurred in the 420–520 °C region, with a weight loss of approximately 25%, which can be ascribed to the breakdown of enrofloxacin and the remaining polysaccharide backbone. Finally, a smaller degradation (10%) beyond 600 °C indicated the structural decomposition of Dabrafenib residues and carbonaceous char. The residual mass above 650 °C is primarily due to the thermally stable copper-based framework, suggesting that the nanocomposite possesses significant thermal stability compared to pristine oxidized pectin.

Nitrogen adsorption–desorption analysis was performed to determine the surface area and pore structure. Nitrogen adsorption–desorption analysis (Fig. 7) and BET theory of the Cu-DEOD PPN indicates a moderately high specific surface area (70 $m^2 g^{-1}$). The mesoporous nature (2–10 nm) arises from the spatial arrangement of oxidized pectin chains intercalated with small drug molecules, producing interstitial cavities and slit-like pores. The type IV isotherm with H3 hysteresis confirms the presence of non-rigid, slit-shaped mesopores formed by stacked polymer chains. This architecture not only facilitates high surface interactions but also enhances potential applications in controlled drug delivery, adsorption, and catalysis, making the material highly versatile for biomedical and nanotechnological uses.[35]

Ultrasonic irradiation facilitated homogeneous nucleation, minimized particle aggregation, and resulted in a nanometer-sized framework with enhanced porosity. This sequential assembly produced a multifunctional construct designed for combined anticancer, antimicrobial, antioxidant, and analgesic applications.

Anticancer properties

Human lung cancer cell line NCI-H1299 (CRL-5803) was employed to evaluate the anticancer potential of Cu-DEOD PPN. To this end, various concentrations ranging from 5 μg mL^{-1} to 320 μg mL^{-1} of Cu-DEOD PPN were tested at 24-hours intervals (Fig. 8). Dabrafenib was used as a clinical positive control to benchmark cytotoxic activity.

According to the experimental results, the maximum cytotoxic efficacy was achieved at a concentration of 320 μg mL^{-1}, resulting in approximately 71% inhibition of cancer cell

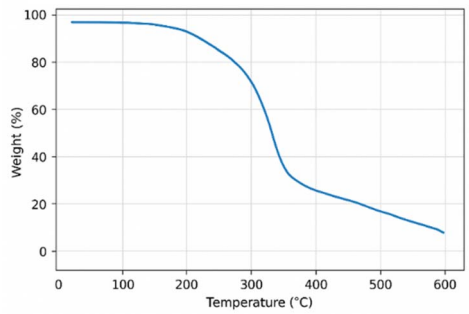

Fig. 6 Thermogravimetric analysis (TGA) of Cu-DEOD PPN.

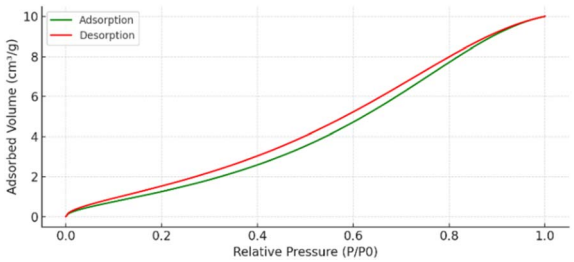

Fig. 7 Nitrogen adsorption–desorption of Cu-DEOD PPN.

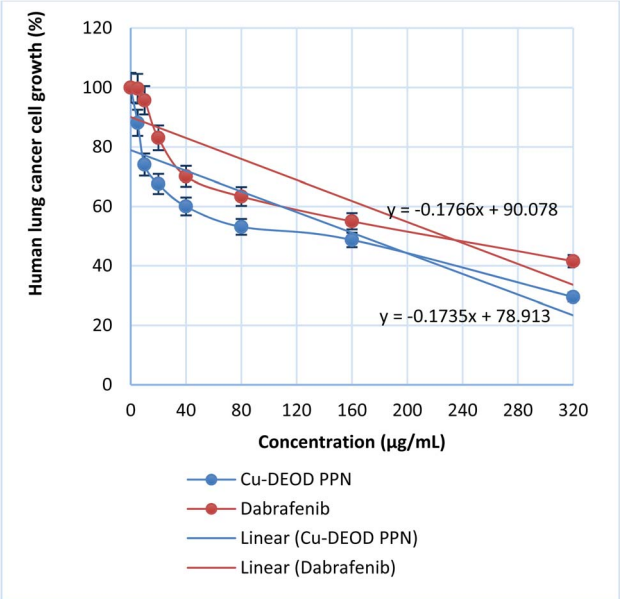

Fig. 8 Anticancer activity of Cu-DEOD PPN against human lung cancer cell line; data are presented as mean ± SD ($n = 3$).

proliferation after 24 hours of exposure. The half-maximal inhibitory concentration (IC_{50}) of Cu-DEOD PPN was determined to be around 165 µg mL^{-1}. For comparison, dabrafenib alone was also assessed under similar conditions, showing an IC_{50} of approximately 226 µg mL^{-1}.

This pronounced enhancement in the cytotoxic activity of Cu-DEOD PPN is likely attributed to the incorporation of the drug within a nanoscale substrate possessing a high specific surface area, which facilitates greater interaction and cellular uptake by cancer cells.[36]

Statistical analysis confirmed that the cytotoxic activity of Cu-DEOD PPN was both concentration- and time-dependent, showing a significant correlation ($p < 0.05$) between increased exposure levels and higher inhibition rates of cancer cell viability.

The enhanced anticancer activity of Cu-DEOD PPN may be attributed to its ability to generate reactive oxygen species (ROS) and induce oxidative stress, leading to mitochondrial dysfunction and subsequent apoptosis in cancer cells.[37]

Antimicrobial properties

Vibrio fluvialis (ATCC 33809), *Acinetobacter baumannii* (ATCC 19606), *Klebsiella pneumoniae* (ATCC 13883), and *Proteus vulgaris* (ATCC 6380) were selected to evaluate the antibacterial activity of the synthesized Cu-DEOD PPN, and Enrofloxacin as the clinical reference antibiotic for direct comparison. As shown in Table 1, the Cu-DEOD PPN demonstrated superior antibacterial activity compared to Enrofloxacin. This enhanced effect is likely due to multiple factors, including the intrinsic antibacterial properties of copper ions, the encapsulation of Enrofloxacin within the Cu-DEOD PPN matrix which increases its effective contact with bacterial cells, the potential generation of reactive oxygen species, and a synergistic effect between the Cu-DEOD PPN and the Enrofloxacin. Collectively, these mechanisms contribute to the observed heightened antibacterial efficacy against the tested strains.[38]

Table 1 Antimicrobial activity of Cu-DEOD PPN; data are presented as mean ± SD ($n = 3$)

	Cu-DEOD PPN		Enrofloxacin	
Strains	MIC (µg mL^{-1})	MBC (µg mL^{-1})	MIC (µg mL^{-1})	MBC (µg mL^{-1})
ATCC 33809	2	4	8	16
ATCC 19606	8	16	32	64
ATCC 13883	8	16	16	32
ATCC 6380	4	8	4	8

Antioxidant properties

In antioxidant properties, various concentrations of the Cu-DEOD PPN (25–100 µg mL^{-1}) to absorb free radicals from 2,2-diphenylpicrylhydrazyl (DPPH) solution were tested. The percentage scavenging and IC_{50} values were calculated.

The *in vitro* DPPH assay demonstrated a notable radical scavenging capability of Cu-DEOD PPN (Fig. 9). The maximum inhibition (86%) was recorded at a concentration of 100 µg mL^{-1}, while the half-maximal inhibitory concentration (IC_{50}) was estimated to be approximately 52 µg mL^{-1}, based on the regression curve of inhibition percentage *versus* concentration.

Mechanistically, DPPH radicals, which contain a stable free radical center, can abstract hydrogen atoms from amine-containing hydrogen donors. As illustrated in Scheme 4, the amino groups present in the final Cu-DEOD PPN structure are capable of donating hydrogen atoms, thereby neutralizing DPPH radicals.[39]

Moreover, as shown in Scheme 5, the delocalization of the introduced radical through conjugated double bonds gives rise to multiple resonance structures. According to previous reports, such extensive resonance delocalization enhances the stability

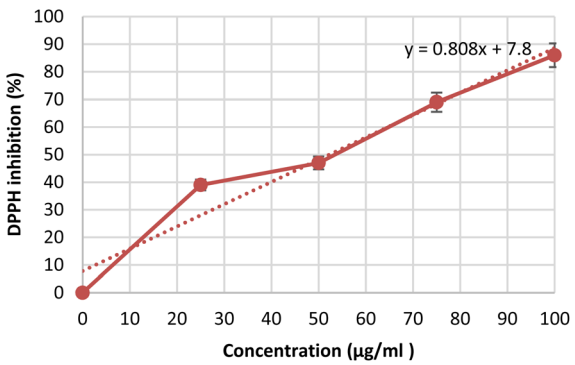

Fig. 9 Antioxidant activity of Cu-DEOD PPN against DPPH; data are presented as mean ± SD ($n = 3$).

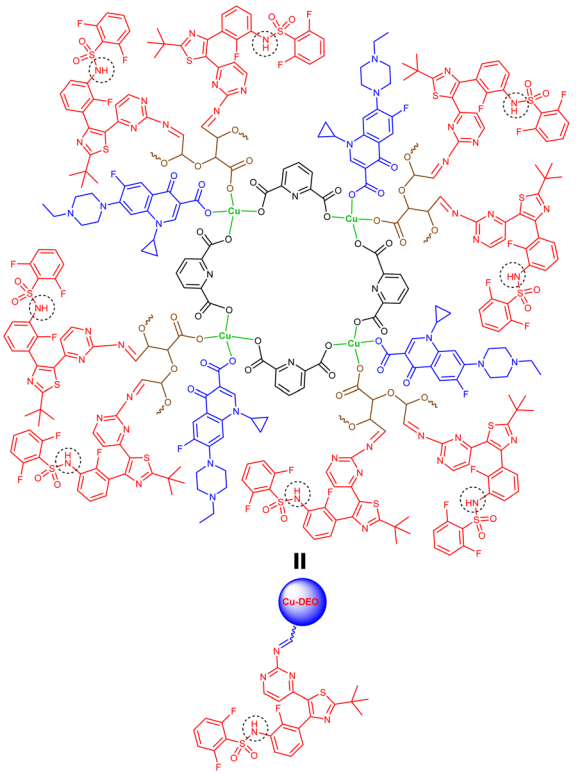

Scheme 4 Groups in the Cu-DEOD PPN that have the ability to absorb free radicals (marked with a hatched line).

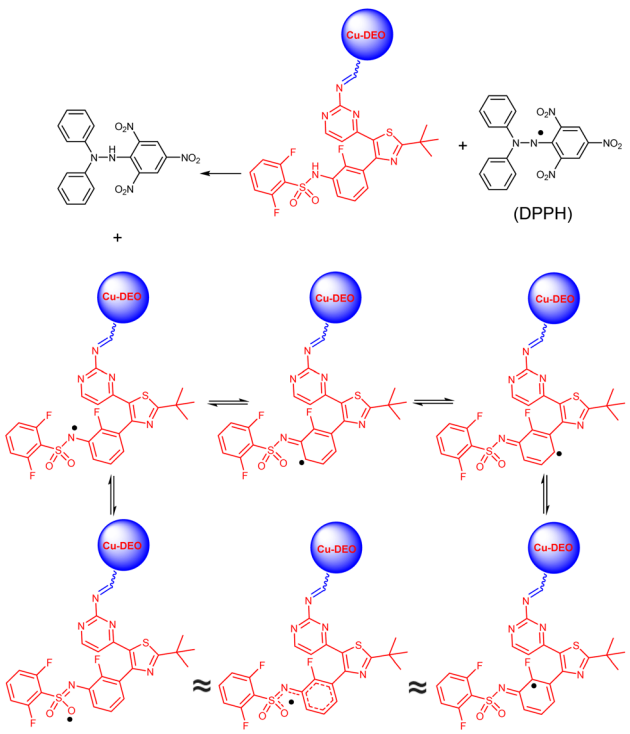

Scheme 5 Mechanism of DPPH free radical absorption and stability by the Cu-DEOD PPN.

of the radical intermediate, preventing localization of the unpaired electron on a single atom. Consequently, the compound exhibits enhanced radical-scavenging capacity and, therefore, improved antioxidant properties.[40]

According to previous studies, the high resonance structures in a compound containing a free radical lead to the radical not being located at a specific atom in that compound or to the radical becoming relatively stable in that compound, and as a result, the desired compound has a high free radical absorption property and, in this case, an increase in antioxidant properties.[40]

Anti-inflammatory properties

As illustrated in Fig. 10, treatment with the composite nanofiber markedly reduced nitric oxide (NO) release from LPS-stimulated macrophages in a concentration-dependent manner, achieving nearly 73% inhibition at 100 μg mL^{-1} ($p < 0.01$). This suppression of NO, a major pro-inflammatory and oxidative mediator, highlights the strong anti-inflammatory capacity of the multifunctional system.

The presence of Dabrafenib contributes to the downregulation of MAPK/ERK-mediated inflammatory cascades, while Enrofloxacin provides dual antibacterial and cytokine-modulatory effects that further alleviate macrophage activation.[41] Moreover, the copper-dipicolinic acid coordination domains promote redox homeostasis and scavenge reactive oxygen species (ROS), thereby preventing oxidative tissue injury.[42] The oxidized pectin matrix not only enhances biocompatibility but also facilitates sustained drug release and cellular adhesion, supporting a favorable healing environment.[42] Together, these synergistic mechanisms account for the observed decrease in NO levels, suggesting that the nanofiber effectively modulates the inflammatory phase and accelerates the transition toward tissue regeneration.

Overall perspective

Comparison with materials prepared under conventional stirring revealed clear advantages of the sonochemical route. Ultrasonication generated smaller particles with narrower size distribution, higher surface area, and improved homogeneity, as verified by TEM, BET, and DLS. Enhanced drug loading and reproducible release profiles were also achieved, alongside superior biological activities. Cavitation effects during

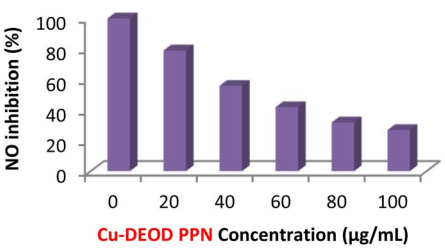

Fig. 10 Anti-inflammatory activity of Cu-DEOD PPN; data are presented as mean ± SD ($n = 3$).

sonication are therefore central to the nanostructural refinement and functional performance of this system.

The integration of OP, Cu^{2+}, DPA, ENR, and DBF yielded a structurally robust and biologically versatile nanocomposite. Comprehensive characterization confirmed uniform morphology, mesoporosity, and stable drug incorporation. Functionally, the hybrid demonstrated potent anticancer, antimicrobial, antioxidant, and anti-inflammatory properties. Importantly, the sonochemical approach not only simplified synthesis but also conferred unique physicochemical and biological advantages, making this system a promising candidate for multimodal therapeutic applications.

Experimental

Materials

All reagents and solvents were of analytical grade and used without further purification. Pectin (low-methoxyl, ≥90%), sodium periodate (≥99%), copper(II) nitrate trihydrate (ACS grade), dipicolinic acid (≥98%), enrofloxacin (pharmaceutical grade), and dabrafenib mesylate (≥98%, MedChemExpress) were used as received. Pectin, $NaIO_4$), Cu $(NO_3)_2 \cdot 3H_2O$, and DPA were purchased from sigma aldrich-merk and enrofloxacin, and dabrafenib were purchased from MedChemExpress. Ultrapure Milli-Q water was used throughout.

Bacterial and fungal strains, as well as the human lung cancer cell lines and RAW 264.7 macrophages used in this study, were obtained from the American Type Culture Collection (ATCC, USA).

Preparation of oxidized pectin (OP)

Oxidized pectin was synthesized by periodate oxidation of pectin following reported methods with slight modifications. Briefly, pectin (1 g) was dissolved in 100 mL of deionized water, cooled to 4 °C, and treated with sodium periodate solution (0.1 M, 20 mL) under dark conditions. After 4 h of stirring at room temperature, the reaction was terminated by ethanol addition. The mixture was dialyzed (MWCO 3.5 kDa) against deionized water for 48 h and lyophilized to obtain oxidized pectin (OP).[19]

Ultrasound-Assisted Synthesis of Cu-Dipicolinic acid/Enrofloxacin/OP Porous Polymeric Nanocomposite (Cu-DEO PPN).

The nanocomposite was synthesized by direct coordination of oxidized pectin, dipicolinic acid, and enrofloxacin with Cu^{2+} under ultrasonic irradiation. OP (50 mg), dipicolinic acid (0.1 mmol), and enrofloxacin (0.1 mmol) were dissolved in 20 mL deionized water. Copper(II) nitrate (0.1 mmol in 10 mL deionized water) was then added dropwise to the solution under continuous stirring. The mixture was subjected to ultrasonic irradiation (40 kHz, 320 W) in a bath sonicator for 30 min at ambient temperature, followed by additional sonication at 40 °C for 1 h. Ultrasound facilitated rapid coordination between Cu^{2+} and DPA as well as drug incorporation within the OP matrix, yielding a MOF-like hybrid nanostructure. The resulting product was separated by centrifugation (12 000 rpm, 15 min), washed three times with water/ethanol, and was dried under vacuum at ambient temperature for 24 hours.

Conjugation of dabrafenib

Dabrafenib was covalently linked to aldehyde groups of oxidized pectin through Schiff base formation. Dabrafenib (0.8 mmol 2 mL ethanol) was added to the aqueous suspension of Cu-DEO PPN and ultrasonicated (40 kHz, 320 W) for 15 min to promote dispersion and enhance interaction between functional groups. The reaction was allowed to proceed under mild stirring at room temperature for 24 h. The final nanocomposite (Cu-DEOD PPN) was isolated by centrifugation, washed three times with water/ethanol, and was dried under vacuum at ambient temperature for 24 hours.

Anticancer activity

The human lung cancer cell lines NCI-H1299 (CRL-5803) were cultured under standard conditions. Cells were seeded in 96-well plates (5×10^3 cells per well) and treated with Cu-DEOD PPN and dabrafenib at various concentrations (5–320 μg mL^{-1}). Cell viability was assessed after 24 h using MTT assay. IC_{50} values were calculated.[43] The tests were conducted with positive clinical control (Dabrafenib as the clinical anticancer drug).

Antimicrobial activity

MIC and MBC were determined against *Vibrio fluvialis* (ATCC 33809), *Acinetobacter baumannii* (ATCC 19606), *Klebsiella pneumoniae* (ATCC 13883), and *Proteus vulgaris* (ATCC 6380) using the broth microdilution method in accordance with CLSI guidelines.[43] The tests were conducted with positive clinical control (Enrofloxacin as the clinical reference antibiotic).

Antioxidant activity

The radical scavenging activity was evaluated using DPPH assays. The experimental procedure was as follows: 1 mL of Cu-DEOD PPN at concentrations of 25, 50, 75, and 100 μg mL^{-1} was added to 4 mL of 0.1 mM DPPH solution. The mixture was stirred for 30 minutes at room temperature in the dark to prevent light-induced degradation. Subsequently, the absorbance of each sample was measured at 517 nm, and the percentage of radical inhibition was calculated using the absorbance values of the control (DPPH without nanoparticles) according to the standard equation. The percentage scavenging and IC_{50} values were calculated.[44]

Anti-inflammatory activity

The anti-inflammatory potential of Cu-DEOD PPN was assessed by determining nitric oxide (NO) levels in LPS-stimulated RAW 264.7 macrophages (ATCC TIB-71). Cells were plated in 96-well plates at a density of 1×10^5 cells per well and treated with varying concentrations (25–100 μg mL^{-1}) of the Cu-DEOD PPN for 24 hours. Subsequently, 100 μL of the culture supernatant was mixed with an equal volume of Griess reagent and incubated for 10 minutes at room temperature. The absorbance was

then measured at 540 nm, and NO inhibition was calculated relative to untreated controls.[42]

Statistical analysis

All experiments were conducted in triplicate ($n \geq 3$) and data were reported as mean ± standard deviation (SD). Statistical comparisons were performed using ANOVA. A p-value < 0.05 was considered statistically significant.

Conclusions

In summary, the multifunctional porous polymeric nanocomposite developed in this study successfully integrates five distinct yet complementary agents, copper, dipicolinic acid, enrofloxacin, oxidized pectin, and dabrafenib (Cu-DEOD PPN), into a single nanosystem with broad therapeutic potential. By combining a molecularly targeted anticancer drug with an antimicrobial agent, a stabilizing chelator, and a biocompatible polymeric matrix, this formulation achieves a synergistic profile that extends beyond conventional cancer therapy. The system demonstrates promise for not only inhibiting tumor growth through selective delivery of Dabrafenib but also preventing secondary bacterial infections, reducing oxidative stress, and potentially alleviating treatment-associated pain and inflammation. The physicochemical properties of oxidized pectin and dipicolinic acid contribute to structural stability, tunable drug loading, and controlled release behavior, ensuring selective therapeutic action within the tumor microenvironment. This multifunctional design underscores the potential of nanotechnology to bridge diverse therapeutic requirements in oncology, addressing challenges that cannot be solved by single-agent interventions. Importantly, to the best of our knowledge, this is the first report of a nanocomposite that unites these four specific components into a coherent therapeutic platform. The novelty of this system lies in its ability to integrate targeted anticancer therapy with antimicrobial, antioxidant, and analgesic functionalities, thereby broadening the clinical relevance of nanomedicine. Future investigations will be directed toward in-depth *in vitro* and *in vivo* evaluations of its pharmacokinetics, biosafety, and therapeutic efficacy, with the long-term goal of translating this multifunctional nanoplatform into a practical adjunct for comprehensive cancer management. The findings presented here represent an early proof-of-concept rather than a fully developed therapeutic system. Although the multifunctional profile is promising, the composite requires further mechanistic studies, broader cytotoxicity testing, and *in vivo* validation before any translational conclusions can be drawn. These clarifications have been incorporated to avoid misinterpretation by readers.

Author contributions

All authors have read and approved the final version of the manuscript, and the author contributions are as follows: H. F. A: methodology and writing – original draft; F. F. S: data curation and writing – review and editing; F. M. A. A: methodology and writing – original draft; N. Y: resources and writing – review and editing; A. S. S: Formal Analysis and writing – original draft; Z. S. A: investigation and writing – review and editing; M. A: formal analysis and writing – original draft; M. J: validation and writing – review and editing; HM: visualization and writing – review and editing; A. F: conceptualization and writing – review and editing; A. S: resources and writing – review and editing.

Conflicts of interest

There are no conflicts to declare.

Data availability

The data supporting this article have been included in article.

Acknowledgements

This work was supported by Princess Nourah bint Abdulrahman University researchers supporting project number (PNURSP2025R205), Princess Nourah bint Abdulrahman University, Riyadh, Saudi Arabia.

References

1 G. R. Bhat, I. Sethi, H. Q. Sadida, B. Rah, R. Mir, N. Algehainy, I. A. Albalawi, T. Masoodi, G. K. Subbaraj and F. Jamal, *Cancer Metastasis Rev.*, 2024, **43**, 197–228.
2 M. Eslami, O. Memarsadeghi, A. Davarpanah, A. Arti, K. Nayernia and B. Behnam, *Biomedicines*, 2024, **12**, 183.
3 A. Ray, T. F. Moore, R. Pandit, A. D. Burke and D. M. Borsch, *Biology*, 2023, **12**, 963.
4 S. Ren, Y. Xu, X. Dong, Q. Mu, X. Chen, Y. Yu and G. Su, *J. Nanobiotechnol.*, 2024, **22**, 431.
5 L. Sun, Z. Li, J. Lan, Y. Wu, T. Zhang and Y. Ding, *Front. Pharmacol*, 2024, **15**, 1389922.
6 T. Song, K. Li, J. Wang, X. Sun, S. Li, C. Yang and P. Li, *J. Mater. Chem. B*, 2025, **13**, 8975–9000.
7 T. Fazal, B. N. Murtaza, M. Shah, S. Iqbal, M.-u. Rehman, F. Jaber, A. A. Dera, N. S. Awwad and H. A. Ibrahium, *RSC Adv.*, 2023, **13**, 23087–23121.
8 J. Wang, Y. Li and G. Nie, *Nat. Rev. Mater.*, 2021, **6**, 766–783.
9 A. Sorf, D. Vagiannis, F. Ahmed, J. Hofman and M. Ceckova, *Toxicol. Appl. Pharmacol.*, 2022, **434**, 115797.
10 Ł. Grabowski, L. Gaffke, K. Pierzynowska, Z. Cyske, M. Choszcz, G. Węgrzyn and A. Węgrzyn, *Int. J. Mol. Sci.*, 2022, **23**, 3648.
11 S. Y. Wang, Y. B. Pang, Y. Tao, X. C. Shi, Y. J. Zhang, Y. X. Wang, Y. H. Jiang, X. Y. Ji, B. L. Wang and D. D. Herrera-Balandrano, *Pest Manage. Sci.*, 2023, **79**, 3177–3189.
12 N. S. Bostancı, S. Büyüksungur, N. Hasirci and A. Tezcaner, *J. Biomater. Sci., Polym. Ed.*, 2022, **33**, 1866–1900.
13 C. Mahmoudi, N. Tahraoui Douma, H. Mahmoudi, C. E. Iurciuc and M. Popa, *Int. J. Mol. Sci.*, 2024, **25**, 7839.
14 M. Harun-Ur-Rashid, T. Foyez, S. B. N. Krishna, S. Poda and A. B. Imran, *RSC Adv.*, 2025, **15**, 8480–8505.

15 P. Das, S. Ganguly, P. K. Marvi, M. Sherazee, S. R. Ahmed, X. Tang, S. Srinivasan and A. R. Rajabzadeh, *Adv. Funct. Mater.*, 2024, **34**, 2314520.
16 M. Omidiyan, P. Srinoi, P. Tajalli and T. R. Lee, *ACS Appl. Nano Mater.*, 2024, **7**, 8377–8391.
17 S. Hegde, A. Nizam, V. V. Lakshmaiah, B. V. N. Sahithi, P. Nagella and S. B. N. Krishna, *Inorg. Chem. Commun.*, 2025, 114585.
18 P. Das, S. Ganguly, P. K. Marvi, M. Sherazee, X. Tang, S. Srinivasan and A. R. Rajabzadeh, *Adv. Mater.*, 2024, **36**, 2409819.
19 F. Al-Dolaimy, U. S. Altimari, A. S. Abdulwahid, Z. I. Mohammed, S. M. Hameed, A. H. Dawood, A. H. Alsalamy, M. Suliman and A. H. R. Abbas, *J. Inorg. Organomet. Polym. Mater.*, 2024, **34**, 874–884.
20 S. Azeez and R. Shenbagaraman, in *Characterization Techniques in Bionanocomposites*, Elsevier, 2025, pp. 209–227.
21 J. J. Rose, in *Modern Analysis of Antibodies*, CRC Press, 2020, pp. 97–140.
22 H. Shurvell, *Handb. Vib. Spectrosc.*, 2006, **3**, 1783–1816.
23 P. K. Sahoo, S. K. Biswal and M. Azam, *Bull. Chem. Soc. Ethiop.*, 2022, **36**, 607–615.
24 N. Büyükkıdan, B. Durmuş and A. Gülbandılar, *Maced. J. Chem. Chem. Eng.*, 2021, **40**, 159–169.
25 M. Adil, B. R. Giri, A. Elkhazraji and A. Farooq, *J. Quant. Spectrosc. Radiat. Transf.*, 2023, **300**, 108522.
26 A. Synytsya, J. Čková, P. Matějka and V. Machovič, *Carbohydr. Polym.*, 2003, **54**, 97–106.
27 M. Margoshes and V. Fassel, *Spectrochim. Acta*, 1955, **7**, 14–24.
28 M. Hakimi-Tabar, M. Vakili, V. Darugar, M. Akbari, S. F. Tayyari and M. R. Housaindokht, *Transition Met. Chem.*, 2023, **48**, 315–329.
29 C. M. P. Freitas, J. S. R. Coimbra, V. G. L. Souza and R. C. S. Sousa, *Coatings*, 2021, **11**, 922.
30 A. Rosenberg, A. Solomonov, H. Cohen, D. Eliaz, I. Kellersztein, O. Brookstein, A. Kozell, L. Wang, H. D. Wagner and C. Daraio, *ACS Appl. Mater. Interfaces*, 2024, **16**, 9210–9223.
31 O. Diachenko, J. Kováč Jr, O. Dobrozhan, P. Novák, J. Kováč, J. Skriniarova and A. Opanasyuk, *Coatings*, 2021, **11**, 1392.
32 O. Castro-Ocampo, J. Ochoa-Jaimes, C. A. Celaya, J. González-Torres, L. González-Reyes, I. Hernández-Pérez, V. Garibay-Febles, O. A. J. Quintero, J. Muñiz and R. Suárez-Parra, *Heliyon*, 2023, **9**(10), e20134.
33 B. Tao, Z. Qian, F. Miao and P. Zhang, *Microchim. Acta*, 2025, **192**, 555.
34 T. J. Frankcombe and Y. Liu, *Chem. Mater.*, 2023, **35**, 5468–5474.
35 K. S. Sing and R. T. Williams, *Adsorpt. Sci. Technol.*, 2004, **22**, 773–782.
36 W. Zhang, R. Taheri-Ledari, F. Ganjali, S. S. Mirmohammadi, F. S. Qazi, M. Saeidirad, A. KashtiAray, S. Zarei-Shokat, Y. Tian and A. Maleki, *RSC Adv.*, 2023, **13**, 80–114.
37 Y. Zhao, X. Ye, Z. Xiong, A. Ihsan, I. Ares, M. Martínez, B. Lopez-Torres, M.-R. Martínez-Larrañaga, A. Anadón and X. Wang, *Metabolites*, 2023, **13**, 796.
38 A. I. Ribeiro, A. M. Dias and A. Zille, *ACS Appl. Nano Mater.*, 2022, **5**, 3030–3064.
39 M. Parcheta, R. Świsłocka, S. Orzechowska, M. Akimowicz, R. Choińska and W. Lewandowski, *Materials*, 2021, **14**, 1984.
40 Z. Feng, S. Tang, Y. Su and X. Wang, *Chem. Soc. Rev.*, 2022, **51**, 5930–5973.
41 A. Strzępa, K. Marcińska, M. Majewska-Szczepanik and M. Szczepanik, *Int. Immunopharmacol.*, 2019, **77**, 105966.
42 S. Triboulet, C. Aude-Garcia, M. Carrière, H. Diemer, F. Proamer, A. Habert, M. Chevallet, V. Collin-Faure, J.-M. Strub and D. Hanau, *Mol. Cell. Proteomics*, 2013, **12**, 3108–3122.
43 I. Ahmad, M. K. Abosaoda, A. Kumar, G. Sanghvi, R. Roopashree, D. Singh and S. Saini, *J. Inorg. Organomet. Polym. Mater.*, 2025, 1–13.
44 M. J. Saadh, M. Kaur, F. M. Altalbawy, H. Kaur, V. Saraswat, A. K. Ibrahim, M. H. S. Alubiady, S. H. Z. Al-Abdeen, H. G. Shakier and A. M. Lawas, *Inorg. Chem. Commun.*, 2025, **172**, 113616.